

Bi@SiO₂ Core@Shell Composites Formation Based on Laser Synthesized Bi Nanoparticles

A. V. Skribitskaya^{a,*}, N. A. Korotkova^b, P. A. Kotelnikova^b, G. V. Tikhonowski^a, A. A. Popov^a,
S. M. Klimentov^a, I. N. Zavestovskaya^c, and A. V. Kabashin^d

^aNational Research Nuclear University MEPhI, Moscow, 115409 Russia

^bShemyakin–Ovchinnikov Institute of Bioorganic Chemistry, Russian Academy of Sciences, Moscow, 117997 Russia

^cLebedev Physical Institute, Russian Academy of Sciences, Moscow, 119991 Russia

^dLP3, Aix Marseille University, CNRS, Marseille, 13288 France

* e-mail: sav1998@list.ru

Received July 14, 2023; revised August 15, 2023; accepted August 15, 2023

Abstract—Present article provides a method of Bi@SiO₂ core@shell nanocomposites obtaining via surface modification of laser-synthesized bismuth nanoparticles with tetraethoxysilane. The SiO₂ shell coating on Bi nanoparticles was demonstrated to form spherical nanoformulations with the mode of size distribution at 250–300 nm. The developed approach is a novel perspective alternative to the traditional methods that allows designing biocompatible Bi-based nanocomposites for the sensitization of multimodal theranostics.

Keywords: nanoparticles, bismuth, surface modification, nanocomposites, laser ablation in liquid

DOI: 10.3103/S1068335623220153

1. INTRODUCTION

Over the past decade, the quantity and quality of basic research in biomedicine has reached a new level, where Bi-based nanomaterials occupy a special place. The highest atomic number among stable elements ($Z = 83$) and unique optical properties motivate the use of Bi-based nanoparticles (NPs) for sensitization of computed tomography and photoacoustic imaging [1, 2], chemotherapy and radiotherapy [3, 4], inhibition of bacterial infections [5], and drug delivery [6, 7]. Traditionally, bismuth NPs are synthesized via complex multi-step chemical reactions using toxic precursors, which often contaminate the NPs surface [8–11]. In this context, pulsed laser ablation in liquid (PLAL) appears to be an attractive alternative approach to produce ultrapure and colloidally stable NPs with controllable properties. High productivity, flexibility, and simplicity of the method determine its wide use in biomedicine, nanophotonics, and power engineering [12–14]. Clinical application of such nanomaterials requires surface modification of NPs with biocompatible compounds to reduce their toxicity and increase accumulation in target areas [12]. The use of silicon dioxide is one of the most effective methods for solving this problem [15]. The uniformity of the morphological and dimensional identity of NPs is a key factor in the synthesis of compounds with a SiO₂ shell [16]. Under such conditions, the PLAL method, which makes it possible to produce NPs with spherical morphology and specified dimensional properties, seems to be an optimal approach [17]. Nanocomposites based on laser-ablated Bi NPs with a biocompatible SiO₂ shell are a new promising compound for sensitizing multimodal theranostics of oncological diseases.

2. MATERIALS AND METHODS

Silicon dioxide shells on Bi NPs were grown using the Stöber method [18]. This method is a widely used sol–gel technique that allows the synthesis of SiO₂ nanoparticles of controllable size and morphology. For the Stöber reaction tetraethoxysilane (TEOS) (C₂H₅O)₄Si (Komponent-reaktiv, Russia), 30% ammonium hydrate (NH₄OH) (Chimmed, Russia), 95% ethyl alcohol (C₂H₅OH), and deionized water (18.2 MΩ cm at 25°C) were used. Bismuth nanoparticles were synthesized by femtosecond pulsed laser ablation in liquid, developed in our previous work [19]. A 3-mm diameter beam from a Yb:KGW laser TETA-10 (Avesta, Russia; wavelength of 1030 nm, pulse duration of 270 fs, pulse energy of 30 μJ, and rep-

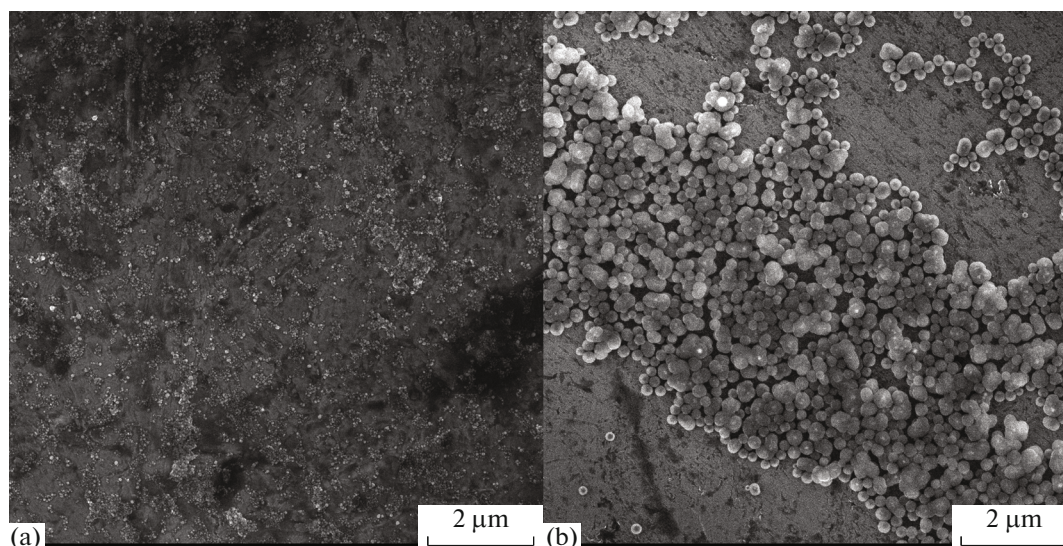


Fig. 1. SEM images of (a) Bi nanoparticles synthesized by PLAL and (b) core@shell structured Bi@SiO₂ nanocomposites.

etition rate of 100 kHz) was focused by a flat-field (F-theta) lens on the surface of a Bi target (GoodFellow, USA, purity 99.5%) immersed in chemically pure acetone. Morphological, dimensional, and structural properties of Bi NPs were studied by using scanning electron microscopy (SEM) (MAIA 3, Tescan, Czech Republic) and energy-dispersive spectrometry (EDS) (X-Act, Oxford Instruments, UK). The hydrodynamic size distribution was obtained by dynamic light scattering (DLS) (Zetasizer ZS, Malvern Instruments, France).

After synthesis in acetone, Bi NPs were transferred to ethanol by centrifugation and solvent exchange. Next, 140 μg of Bi NPs was dissolved in 9 mL of ethanol. Then, 600 μL of deionized water and 500 μL of ammonia hydrate were added to the colloid. Under the constant stirring, 1 mL of 45 mM tetraethoxysilane was added dropwise to the resulting solution with NPs. The final colloid was placed in a laboratory rotator for 16 hours at the room temperature, after that the nanocomposites were washed in ethanol by triple centrifugation for 15 min at 5000g.

3. RESULTS AND DISCUSSION

Analysis of SEM data clearly indicates the formation of Bi NPs and Bi@SiO₂ nanocomposites with close-to-spherical morphology, which is typical of PLAL (Fig. 1). Also, SEM images of Bi@SiO₂ nanocomposites display a clearly visible core@shell structure, where bright centers correspond to the cores of Bi nanoparticles, and the less contrasting surface layer corresponds to the SiO₂ shell (Fig. 1b).

The results of characterization of dimensional properties of laser-ablated Bi NPs and Bi@SiO₂ nanocomposites are presented in Figs. 2a and 2b, respectively. Size distributions of the prepared nanomaterials conforms to the lognormal law. The size distribution mode of the original bismuth NPs is in the range from 30 to 40 nm, while the distribution mode of nanocomposites is in the range from 250 to 300 nm. Differences in the distributions of the Feret diameter and hydrodynamic diameter are due to the specifics of the DLS measurements. The DLS method is not able to separate the presence of small NPs from the background of larger ones, which affects the broadening of the size distribution and a shift of the mode towards larger sizes.

In addition, the Stöber reaction produced both composites with Bi NPs core and SiO₂ shell and pure SiO₂ NPs. These nanoformulations cannot be completely separated from Bi@SiO₂ nanocomposites. However, individual SiO₂ nanoparticles are easily identified using SEM. This circumstance made it possible not to take SiO₂ NPs into account when plotting the size distribution of nanocomposites with SEM images, but it affected the results of DLS measurements. To confirm the formation of SiO₂ shell on the surface of laser-ablated Bi NPs, we additionally analyzed the chemical structure of nanocomposites using energy-dispersive spectroscopy. The results of EDS analysis of Bi NPs and Bi@SiO₂ nanocomposites are presented in Fig. 3. The data were normalized to the signal from Bi. The study of the compositional char-

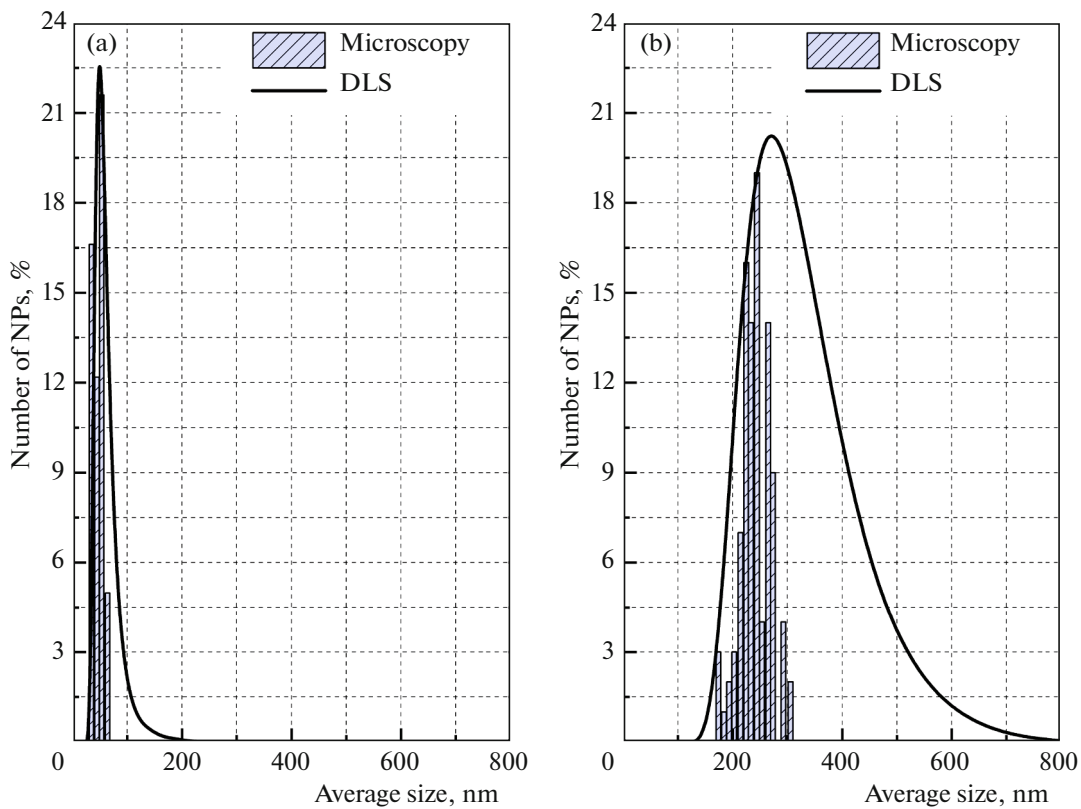


Fig. 2. Size distributions of (a) laser-ablated Bi nanoparticles and (b) Bi@SiO₂ nanocomposites.

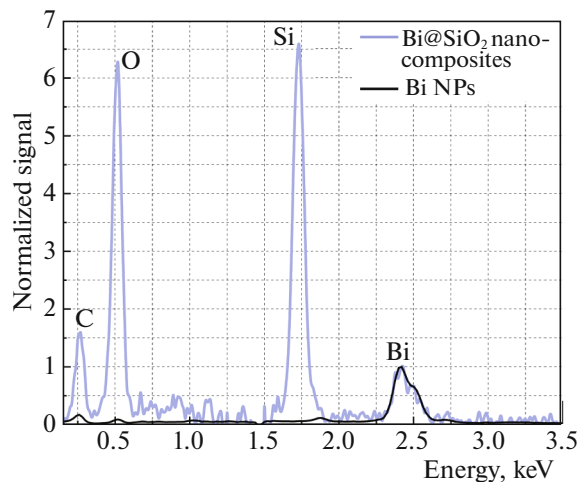


Fig. 3. Results of EDS analysis of laser-ablated Bi nanoparticles and Bi@SiO₂ nanocomposites.

acteristics of the synthesized NPs reliably confirmed the presence of Bi in both types of nanomaterials. The presence of Si and O in the composition of nanocomposites, which are the main elements of the shell, was also detected. The presence of oxygen in the composition of the initial Bi NPs is due to weak oxidation of the NPs surface during laser ablation, while the presence of carbon for both types of NPs can be due to organic contamination of the SEM vacuum chamber.

The EDS analysis together with the obtained SEM images confirms the formation of core@shell structured nanocomposites with core of laser-synthesized Bi NPs and shell of SiO₂.

4. CONCLUSIONS

Core@shell structured nanocomposites were prepared by chemical modification of laser-synthesized Bi NPs surface using tetraethoxysilane. The use of the PLAL method made it possible to obtain Bi NPs with relatively uniform morphological and size characteristics and with a size distribution mode in the range of 30–40 nm. The synthesized NPs acted as nucleation centers for biocompatible SiO₂ shells during the Stöber reaction. Using SEM and EDS, the formation of Bi@SiO₂ nanocomposite structures with close-to-spherical morphology and size distribution mode in the range from 250 to 300 nm was reliably demonstrated. The use of a biocompatible SiO₂ modification will not only reduce the toxicity of the Bi core, but also preserve all the original multimodal theranostic properties.

FUNDING

The work was supported by the Ministry of Science and Higher Education of the Russian Federation (agreement no. 075-15-2021-1347 and grant no. FSWU-2023-0070).

CONFLICT OF INTEREST

The authors declare that they have no conflicts of interest.

REFERENCES

1. Yu, X., Li A., Zhao, C., Yang, K., Chen, X., and Li, W., *ACS Nano*, 2017, vol. 11, p. 3990.
2. Zelepukin, I.V., Ivanov, I.N., Mirkasymov, A.B., Shevchenko, K.G., Popov, A.A., Prasad, P.N., Kabashin, A.V., and Deyev, S.M., *J. Controlled Release*, 2022, vol. 349, p. 475.
3. Kowalik, M., Masternak, J., and Barszcz, B., *Curr. Med. Chem.*, 2019, vol. 26, p. 729.
4. Alqathami, M., Blencowe, A., Geso, M., and Ibbott, G., *J. Biomed. Nanotechnol.*, 2016, vol. 12, p. 464.
5. Salari, S.S., Gholipour, A., Qubais, S.B., Al-Naqeeb, B.Z.T., Abdullah AL-Tameemi, N.M., Nassar, M.F., Amini, P., Yasamineh, S., and Gholizadeh, O., *World J. Microbiol. Biotechnol.*, 2023, vol. 39, p. 190.
6. Wei, X., Shang, Y., Zhu, Y., Gu, Z., and Zhang, D., *Smart Medicine*, 2023, vol. 2, e20220009.
7. Szostak, K., Ostaszewski, P., Pulit-Prociak, J., and Banach, M., *Pharm. Chem. J.*, 2019, vol. 53, p. 48.
8. Yang, Y., Ouyang, R., Xu, L., Guo, N., Li, W., Feng, K., Ouyang, L., Yang, Z., Zhou, S., and Miao, Y., *J. Coord. Chem.*, 2015, vol. 68, p. 379.
9. Yang, C., Guo, C., Guo, W., Zhao, X., Liu, S., and Han, X., *ACS Appl. Nano Mater.*, 2018, vol. 1, p. 820.
10. Ibrahim, S., Ntomprougkidis, V., Goutte, M., Monier, G., Traikia, M., Andanson, J.M., and Bonnet, P., Bousquet, A., *Nanoscale*, 2023, vol. 15, p. 5499.
11. Vazquez-Munoz, R., Arellano-Jimenez, M.J., and Lopez-Ribot, J.L., *Methods X*, 2020, vol. 7, p. 100894.
12. Zelepukin, I.V., Popov, A.A., Shipunova, V.O., Tikhonowski, G.V., Mirkasymov, A.B., Popova-Kuznetsova, E.A., Klimentov, S.M., Kabashin, A.V., and Deyev, S.M., *Mater. Sci. Eng. C*, 2021, vol. 120, p. 111717.
13. Tselikov, G.I., Ermolaev, G.A., Popov, A.A., Tikhonowski, G.V., Panova, D.A., Taradin, A.S., Vyshevyy, A.A., Syuy, A.V., Klimentov, S.M., Novikov, S.M., Evlyukhin, A.V., Kabashin, A.V., Arsenin, A.V., Novoselov, K.S., and Volkov, V.S., *Proc. Natl. Acad. Sci. U. S. A.*, 2022, vol. 119, p. 2208830119.
14. Farooq, S., Vital, C.V., Tikhonowski, G., Popov, A.A., Klimentov, S.M., Malagon, L.A., de Araujo, R.E., Kabashin, A.V., Rativa, D., *Sol. Energy Mater. Sol. Cells*, 2023, vol. 252, p. 112203.
15. Li, Z., Fan, X., Liu, J., Hu, Y., Yang, Y., Li, Z., Sun, Y., Chen, C., and Yu, M., *Nanomedicine*, 2018, vol. 13, p. 2283.
16. Lai, B.H. and Chen, D.H., *Acta Biomater.*, 2013, vol. 9, no. 7, p. 7556.
17. Tikhonovsky, G.V., Popov, A.A., Kurinnaya, A.A., Garmash, A.A., Gromushkina, E.V., Zavestovskaya, I.N., Klimentov, S.M., and Kabashin, A.V., *Bull. Lebedev Phys. Inst.*, 2022, vol. 49, p. 180. <https://doi.org/10.3103/S1068335622060070>
18. Stober, W., Fink, A., and Bohn, E., *J. Colloid Interface Sci.*, 1968, vol. 26, p. 62.
19. Bulmahn, J.C., Tikhonowski, G.V., Popov, A.A., Kuzmin, A., Klimentov, S.M., Kabashin, A.V., and Prasad, P.N., *Nanomaterials*, 2020, vol. 10, p. 1463.

Translated by I. Ulitkin

Publisher's Note. Allerton Press remains neutral with regard to jurisdictional claims in published maps and institutional affiliations.